# THE INFLUENCE OF INTERGRANULAR MICROCRACKS ON THE PETROPHYSICAL PROPERTIES OF SANDSTONE - EXPERIMENTS TO QUANTIFY EFFECTS OF CORE DAMAGE

P.M.T.M. Schutjens, M. Hausenblas, M. Dijkshoorn, J.G. van Munster
Department of Geophysics and Petrophysics, Shell Research, P.O.Box 60,
2280 AB Rijswijk, The Netherlands

*Abstract*

Coring-induced alterations of rock microstructure may change the petrophysical properties to such an extent that the data are no longer representative of the in-situ reservoir rock behaviour. Literature results suggest that stress relief associated with coring is accompanied by strain relaxation caused by the formation and opening of cracks between adjacent grains. In the present experiments, this type of core damage was simulated in Bentheim sandstone by heating it to 650°C for 24 hours. The observed increase of the average grain boundary width was quantified and was found to decrease the ultrasonic compressional wave velocity by about 25%. It also increased the volumetric static compressibility by about 30% at stresses less than 60 bar and decreased the electrical resistivity by about 10%. The grain boundaries in a reservoir sandstone cored from a gas reservoir showed widths similar to those of the temperature treated outcrop sandstone. This suggests that the grain boundaries in the reservoir sandstone may have opened during or after coring, thereby altering the rock's petrophysical properties.

*Introduction*

An essential assumption for the application of laboratory results to reservoir studies is that the petrophysical properties of core samples are similar to those of the in-situ reservoir rock. However, the validity of this assumption is questionable in view of observations that coring rock from the deep subsurface is accompanied by a time-dependent increase in the core size. This size increase, known as strain relaxation, is found to be greatest in the maximum in-situ stress direction and least in the minimum in-situ stress direction [1-3]. Ultrasonic wave velocity measurements [4-6] combined with acoustic emission data [7-9] suggest that an important mechanism in the strain relaxation process is the development of an anisotropic orientation distribution of microcracks within the core, reflecting the anisotropy of the in-situ reservoir stress state. Most of these microcracks are probably intergranular (i.e., in between adjacent grains), since grain contacts are relatively weak zones in the load-bearing grain framework, particularly in the absence of cement. Such microcracks may not only affect ultrasonic wave velocity, but also influence other petrophysical properties like

static compressibility, electrical resistivity and permeability [10-12], casting doubt on the validity of the assumption stated above of similar petrophysical behaviour of cored and uncored reservoir rock. It is therefore important to gain insight into the formation mechanism, location and morphology of intergranular microcracks in cored rock, and to investigate how these microcracks behave like regions of "core damage", changing the petrophysical properties of the rock. Experimental studies into coring-induced alteration of the rock microstructure are scarce [13, 14]. This contribution aims to gain insight in core damage through laboratory experiments on consolidated outcrop. It focuses on microstructural analysis of the manifestations of core damage and its influence on petrophysical properties.

*Experimental method*

We attempted to simulate core damage by a heat treatment of outcrop sandstone. Vertical cylindrical samples were drilled from a block of well-consolidated Bentheim outcrop sandstone. The Bentheim sandstone is a homogeneous, quartz-rich sandstone with less than 3% clay. The diameter of the quartz grains ranges from 50 μm to 500 μm, but most grains are in the range 200 - 400 μm. No sedimentary layering was visible with the naked eye. However, optical and scanning electron microscopy (SEM) of vertical sections through the rock showed a layering with a 5-10° dip, defined by a grain shape preferred orientation.

Eight samples (numbered MD2 to MD9) were selected for the measurement program. The porosity of the samples at ambient conditions was determined by the buoyancy method. Four Bentheim samples (MD2, MD3, MD4, MD5) were heated to 650°C (± 10°C) within about two hours, maintained at this temperature for 24 hours, and then cooled to room temperature within about two hours. The colour of the heated samples changed from soft yellow-white to reddish white, indicating oxidation of iron-bearing minerals. A permanent weight loss in the range 0.05 g to 0.1 g was measured, probably due to loss of water bound in the crystal structure of clays and micas. Furthermore a permanent elongation of the sample of 0.2 - 0.3% occurred in the axial direction and of 0.1 - 0.2% in the radial direction and the porosity increased from about 23.7% before heating to about 24.3% afterwards. The heating-induced weight reduction of the samples can only account for up to one third of the average observed porosity increase. A study performed on SEM photomicrographs revealed that the additional porosity increase is caused by an increase in average grain boundary width at the contacts between quartz grains (Fig. 1). Figure 2 shows histograms of the grain boundary thickness in both non-heated and heated Bentheim sandstone measured from SEM photomicrographs of randomly picked quartz-quartz grain contacts taken at a magnification factor of 1600 (Figs. 2a and 2b). All photographs were taken from 2D sections oriented parallel to the cylindrical axis of the samples. Grain boundary widths were measured only at locations where the shape of the boundaries of adjacent grains was similar, assuming that these boundaries once formed a closed grain-to-grain

contact. The range of grain boundary widths increases from 0.1 to 0.3 μm in the non-heated sandstone to between 0.1 and 0.9 μm in the heated sandstone, independent of the magnification factor. This widening of grain boundaries and the associated increase in average porosity are probably caused by different thermal expansion of quartz grains in contact with each other, inducing small displacements of the grains relative to each other that have not been reversed upon cooling.

*Ultrasonic wave velocity*

The ultrasonic wave velocity was measured on samples MD2 (wet) and MD3 (dry), before and after the heat treatment, and on the non-heated samples MD8 and MD9. In Figure 3 (a, b), the velocity data are presented as a function of the intersection of the wave propagation direction with the dipping layering. The zero degrees point corresponds to the azimuth of the dipping layering. Figure 3a shows the ultrasonic compressional wave velocity ($v_p$) data for the samples before heat treatment. The sinusoidal shape of the data points reflects the influence of the layering on the diametrically measured ultrasonic wave velocity, and leads to a 6% anisotropy in the velocity measured across the sample diameter. The lowest $v_p$ values were measured parallel to the azimuth of the layering; the highest $v_p$ values were measured parallel to the strike of the layering. The ultrasonic shear wave velocity ($v_s$) before and after heating was measured on the dry sample MD3 only. Figure 3b shows the $v_p$ data measured along the diameter of the samples MD2 and MD3 before and after the heat treatment. The heat treatment decreased the average $v_p$ of sample MD3 from about 3.06 km/s to about 2.21 km/s when measured under water-saturated conditions, and from about 2.57 km/s to about 1.47 km/s when measured under laboratory-dry conditions. The shear wave velocity decreased by more than a factor of two due to the heat treatment. Note also the reduction of the diametrical ultrasonic velocity anisotropy in the water-saturated samples from about 6% before heating to about 3% afterwards (Fig. 3b). Under dry conditions, the reduction in the anisotropy of $v_p$ is even more pronounced.

*Volumetric static compressibility*

The heated samples MD2, MD4 and MD5 and the non-heated samples MD6, MD7 and MD9 were saturated with water containing 80 g/l dissolved NaCl. They were compacted isostatically to 700 bar with the pore fluid drained to 1 atmosphere. The volume change of the samples was calculated from measurements of the amount of pore fluid expelled from the compacting sample and used to compute the volumetric compressibility (Cb) and the porosity of the sample as a function of isostatic confining stress (Pc). The results are shown in Figs. 4 and 5, respectively. Note the non-linear decrease of Cb and porosity with increasing Pc. At Pc < 60 bar, the Cb of the heated samples is higher than that of the non-heated samples. This difference becomes insignificant at stresses greater than 60 bar. Figure 5 shows the decrease in porosity of the non-heated and the heated samples as a function of the isostatic confining stress.

Below a Pc of 60 bar, the porosity reduction with increasing stress is somewhat stronger in the heated samples than in the non-heated ones. In the range 60 to 700 bar, the data trends indicate a similar porosity reduction: The average volumetric strain of the heated samples at 700 bar is 19.4 millistrain (Table 1), while the average volumetric strain of the non-heated samples at 700 bar is 18.2 millistrain. However, the unloading behaviour from 700 bar to 1 atmosphere is very different.

**Table 1: Comparison of compaction behaviour**

| Sample | Treatment | $\phi_0$ [% Vb] | $\phi_{700}$ [% Vb] | $\varepsilon_{v,700}$ [millistrain] | $\phi_0'$ [%] | $\varepsilon_v'$ [millistrain] | inel/el |
|---|---|---|---|---|---|---|---|
| MD2 | heated | 24.1 | 22.6 | 19.1 | 23.6 | 6.1 | 0.46 |
| MD4 | heated | 24.1 | 22.6 | 20.6 | 23.6 | 7.1 | 0.53 |
| MD5 | heated | 24.2 | 22.8 | 18.6 | 23.6 | 7.3 | 0.65 |
| MD6 | non- heated | 23.7 | 22.3 | 18.0 | 23.5 | 2.6 | 0.17 |
| MD7 | non- heated | 23.5 | 22.1 | 17.3 | 23.3 | 2.5 | 0.17 |
| MD9 | non- heated | 23.3 | 21.8 | 19.4 | 23.2 | 1.4 | 0.08 |

Explanation of symbols:

| | |
|---|---|
| $\phi_0$ | Porosity before compaction at atmospheric conditions |
| $\phi_{700}$ | Porosity at Pc=700 bar |
| Vb | Bulk volume |
| $\varepsilon_{v,700}$ | Volumetric strain at Pc=700 bar, calculated using $\varepsilon_v = (\phi_0 - \phi_t)/(1 - \phi_t)$, where $\varepsilon_v$ is the volumetric strain, $\phi_0$ is the starting porosity (atmospheric conditions) and $\phi_t$ is the porosity at a given stress; 1 millistrain = $(\Delta V/V_0)x1000$ |
| $\phi_0'$ | Porosity after unloading to atmospheric conditions |
| $\varepsilon_v'$ | Inelastic volumetric strain after unloading to atmospheric conditions |
| inel/el | Ratio of inelastic versus elastic compaction |

The heated samples show a strain recovery of about 13 millistrain (ca. 0.4 porosity units) during unloading from 700 bar to 1 atmosphere, leaving an inelastic deformation of only about 7 millistrain (see Table 1). In contrast, the non-heated samples show an almost complete strain recovery of about 16 millistrain (ca. 0.6 porosity units), yielding a permanent volumetric strain of about 2 millistrain. The heating-induced increase in grain boundary width in the heated samples apparently enhances the inelastic (permanent) component of the compaction: In the non-heated samples the ratio of inelastic versus elastic compaction is about 0.55, whereas in the non-heated samples this ratio is about 0.14 (Table 1).

*Electrical resistivity*

During the loading cycle, the electrical resistivity of the sample was measured at regular stress intervals. The resistivity of the formation water was measured separately. Figure 6 shows the formation resistivity factor (FRF, which is defined as the resistivity of a fluid-saturated sample divided by the resistivity of its pore fluid) as a function of Pc. The FRF of the heated samples is consistently lower than that of the non-heated samples. Also note the non-linear increase in FRF with increasing Pc in all experiments. Below 60 bar, the heated samples (that probably contained many initially open grain boundaries) show a stronger increase in FRF with increasing Pc than the non-heated samples. Above 60 bar, the two data-groups exhibit a similar trend.

*Interpretation*

The ultrasonic wave velocity data demonstrate the potential of ultrasonic velocity measurements for detecting changes in the average grain boundary width. The compressibility and porosity data show that this subtle change in the microstructure can control compaction at low stress levels. The increase in the average grain boundary width appears to increase the volumetric static compressibility by up to 30% at stresses below 60 bar and increase the ratio of inelastic versus elastic strain during volumetric (3D) compaction by about a factor of 4. Microstructural variation is also identified as the cause of the difference in FRF between heated and non-heated samples. The FRF of the heated samples is consistently lower than that of the non-heated material. This is partly due to the heated material having a higher porosity at a given stress than the non-heated material. Partly it is probably also due to the heated material having a lower solid-solid grain contact surface area per unit volume of rock than the non-heated material (see Figs. 1a and 1b). The difference in the non-linear increase in FRF with increasing Pc at low stresses (Fig. 6) can be explained by a different non-linear increase of the solid-solid grain contact surface area per unit volume with increasing Pc.

Summarising, the heating-induced change in average grain boundary width of the Bentheim sandstone influences the ultrasonic wave velocity measured at one atmosphere, and the volumetric compressibility and electrical resistivity at isostatic stresses lower than 60 bar. At stresses higher than 60 bar, the changes in volumetric compressibility and electrical resistivity with increasing stress become similar for non-heated and heated samples. This suggests that the heating-induced change in average grain boundary width has been largely restored at stresses higher than 60 bar, possibly because in the stress range 1 to 60 bar the relatively "open" grain boundaries closed more rapidly with increasing grain contact stress than the relatively "closed" grain boundaries.

*Application of the present results to reservoir rock*

The present experiments on Bentheim sandstone demonstrate that opening previously closed grain boundaries can influence such petrophysical properties as $v_p$, $v_s$, Cb and FRF of well-consolidated quartz-rich sandstone. The results also indicate that the influence of this type of core damage on compressibility and resistivity is probably limited to relatively low stresses (< 60 bar) and is likely not to be observed any more when in-situ stress conditions on the core sample are restored (see also [15]).

With these observations in mind, a SEM study was conducted on sandstone cored from a gas reservoir (retrieval depth about 3350 m). This reservoir sandstone resembles the Bentheim outcrop sandstone in terms of composition (> 90% quartz), porosity (about 22%), grain shape (rounded to elliptical) and grain contact morphology (abundant tangential contacts), but has a larger spread in grain size (100 - 1000 μm) than the Bentheim sandstone (50 to 500 μm). In the reservoir sandstone, no evidence was found for abundant intragranular microcracks, which are often associated with coring-induced alterations to the in-situ microstructure of reservoir rock [15,16]. However, many "open" grain boundaries were visible (Fig. 7) which seem to have a similar morphology to those in the heated Bentheim samples (see Fig. 1b). Furthermore, the reservoir sandstone showed some evidence of intergranular displacements of a few microns in a direction approximately parallel to the grain boundaries. Grain boundary widths were measured at 40 randomly picked adjacent grains at locations showing similar grain surface shapes, and found to fall in the range 0.2 to 2.8 μm (Fig. 8a). The spread in the grain boundary width reduces to a range of 0.2 - 1.6 μm when only the boundary widths between relatively small grains are measured (Fig. 8b, grain size reservoir sandstone: 100 - 400 μm, similar to the grain size range of the Bentheim sandstone). The fact that most grain boundaries in the reservoir sandstone samples are even wider than in the heated Bentheim outcrop samples suggests that the microstructure of the reservoir rock may have changed during and/or after coring from the reservoir.

To what extent the inferred coring-induced alteration of the microstructure of the reservoir sandstone may have changed a petrophysical property like uniaxial compressibility is unknown. Despite the apparent textural and lithological similarity between Bentheim outcrop sandstone and the reservoir sandstone, care should be taken when attempting to apply the Bentheim results to quantify this influence. There may be subtle differences between the two rocks that could also exert a strong influence on petrophysical properties, such as the size, shape and sorting of the load-bearing grains, the contact surface area between adjacent grains per unit volume, and the abundance and the structural position of cement and clay with respect to the load-bearing grains [17].

*Conclusions and Recommendations*

- A heat-treatment of Bentheim sandstone increased the porosity and was associated with an increase of the boundary width between adjacent grains. The heating-induced change in microstructure decreased the ultrasonic compressional wave velocity by about 25%, increased the volumetric static compressibility by about 30% (at stresses < 60 bar) and decreased the electrical resistivity by about 10%.
- The grain boundaries in sandstone cored from a gas reservoir showed widths similar to those of the experimentally heated outcrop sandstone. This suggests that the grain boundaries in the reservoir sandstone may have opened during or after coring, which possibly altered the rock's petrophysical properties.
- The influence of core damage on the petrophysical properties of reservoir rock can only be quantified with confidence by comparing laboratory measurements with wireline petrophysical data obtained on the same type of rock in the reservoir, and then only if the reservoir rock is under a known state of stress and if it is not damaged by the drilling process.
- In view of the common uncertainty concerning the reservoir (horizontal) stress state and the extent of core damage, an improved understanding of the influence of core damage on the petrophysical measurements should come from basic laboratory experiments performed under well-controlled stress conditions and using homogeneous starting material with a simple microstructure.

*Acknowledgements*

F.K. Lehner suggested to heat the Bentheim sandstone in order to produce "core damage" microstructures. The authors thank Shell Internationale Research Maatschappij B.V. for granting the permission to publish this paper.

*References*

[1] Teufel, L.W.: Determination of in-situ stress from anelastic strain recovery measurements of oriented core. Paper SPE 11649 presented at the 1983 SPE/DOE Symp. on Low Permeability Reservoirs, Denver, 14-16.

[2] Engelder, T. and Plumb, R.: Changes in in-situ ultrasonic properties of rock on strain relaxation. Int. J. Rock Mech. Min. Sci. & Geomech. Abstr. (1984) 21, No 2, 75-82.

[3] Wolter, K.E. and Berckhemer, H.: Time-dependent strain recovery of cores from the KTB - Deep drill hole. Rock Mechanics and Rock Engineering (1989) 22, 273-287.

[4] Ren, N.-K. and Hudson, P.J.: Predicting the in-situ state of stress using Differential Wave Velocity Analysis. Proc. 26th US Symposium on Rock Mechanics, Rapid City, 26-28 (1985) Assoc. Eng. Geol., 1235-1244.

[5] Sayers, C.M. van Munster, J.G. and King, M.S.: Stress-induced ultrasonic anisotropy in Berea sandstone. Int. J. Rock Mech. Min. Sci. & Geomech. Abstr. (1990a) 27, 429-436.

[6] Sayers, C.M. and van Munster, J.G.: Microcrack-Induced seismic anisotropy of sedimentary rocks. J. Geophys. Res. (1990b) 96, Nº B10, 16529-16533.

[7] Hughson, D.R. and Crawford, A.M.: Kaiser effect gauging: A new method for determining pre-existing in-situ stress from an extracted core by acoustic emissions. Proceedings of the International Symposium on Rock Stress and Rock Stress Measurements, Stockholm (September, 1986) 359-369.

[8] Momayez, M. and Hassani, F.P.: Application of Kaiser effect to measure in-situ stresses in underground mines. In: Tillerson & Wawesik (eds): Proceedings of the 33rd U.S. Symposium on Rock Mechanics, Balkema, Rotterdam (1992) 979-988.

[9] Holcomb, D.J. Observations of the Kaiser effect under multiaxial stress states: implications for its use in determining in-situ stress. J. Geophys. Res. (1993) 20, 2119-2122.

[10] Sayers, C.M.: Orientation of microcracks formed in rocks during strain relaxation. Technical Note Int. J. Rock Mech. Min. Sci. & Geomech. Abstr. (1990c) 27, 437-39.

[11] Morita, N., Gray, K.E., Fariz, A.A.S. and Jogi, P.N.: Rock property changes during reservoir compaction. Paper SPE Formation Evaluation (Sept., 1992), 197 - 205. Paper SPE 13099 first presented at the 1984 SPE Annual Technical Conference and Exhibition, Houston.

[12] David, C., Wong, T.-F., Zhu, W. and Zhang, J.: Laboratory measurement of compaction-induced permeability change in porous rocks: implications for the generation and maintanance of pore pressure excess in the crust. Pure and Applied Geophysics (1995), 143, 425-457.

[13] Holt, R.M. and Kenter, C.J.: Laboratory simulation of core damage induced by stress release. KSEPL report, investigation nr. 6DR/1281. Submitted to the 33rd Rock Mechanics Symposium, Santa Fe, USA 1992.

[14] Holt, R.M., Brignoli, M., Fjaer, E., Kenter, C.J. and Unander, T.E.: Core damage effects on compaction behaviour. Paper presented at EUROCK '94: An SPE/ISRM Conference: Rock mechanics in Petroleum Engineering, Delft, The Netherlands, August 29-31, 1994.

[15] Schutjens, P.M.T.M., Ruig, H. de, Sayers, C.M., Munster, J.G. van and Whitworth, J.L.: Compressibility measurement and acoustic characterisation of quartz-rich consolidated reservoir rock (Brent Field, North Sea). Paper presented at EUROCK '94: An SPE/ISRM Conference: Rock mechanics in Petroleum Engineering, Delft, The Netherlands, August 29-31, 1994.

[16] Farquhar, R.A., Smart, B.D.G., Crawford, B.R., Todd, A.C. & Tweedie, J.A.: Mechanical properties analysis: The key to understanding petrophysical properties stress sensitivity. Society of Core Analysts Conference Paper 9321, (1993).

[17] Vernik, L. and Nur, A.: Petrophysical classification of siliciclastics for lithology and porosity prediction from seismic velocities. Am. Assoc. Petrol. Geol. Bull. 76, Nº 9 (Sept. 1992), 1295-1309.

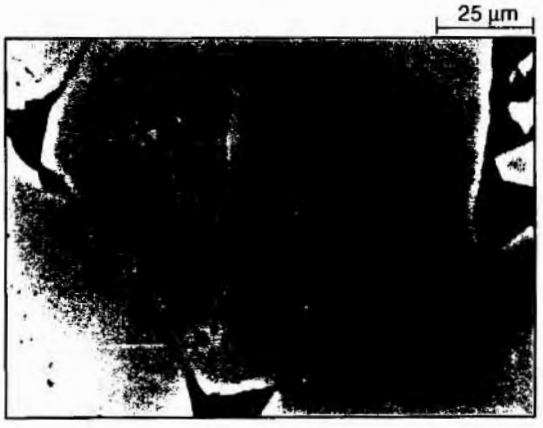


**Fig. 1a Typical "closed" grain boundary morphology between quartz grains in non-heated Bentheim sandstone.**

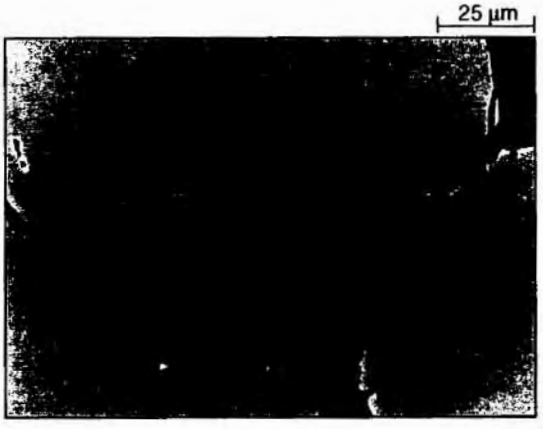


**Fig. 1a Typical "open" grain boundary morphology in heated Bentheim sandstone.**

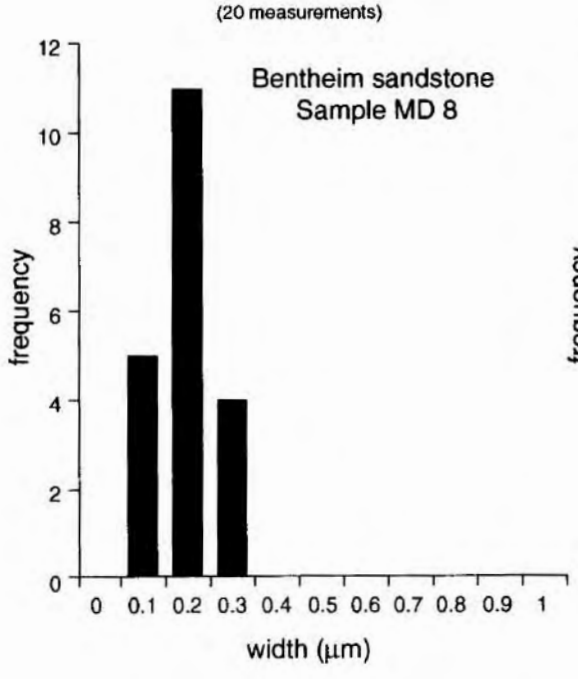


**Fig. 2a Grain boundary width of non-heated Bentheim sandstone sample MD8, measured from SEM photomicrographs.**

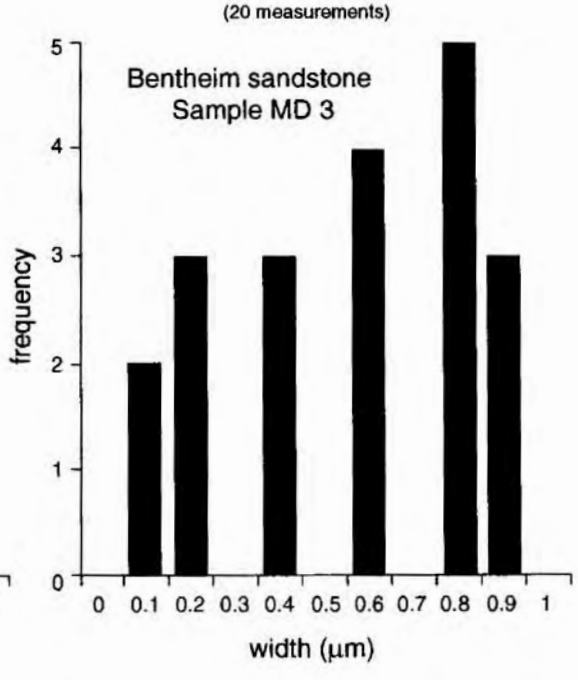


**Fig. 2b Grain boundary width of heated Bentheim sandstone sample MD3, measured from SEM photomicrographs.**

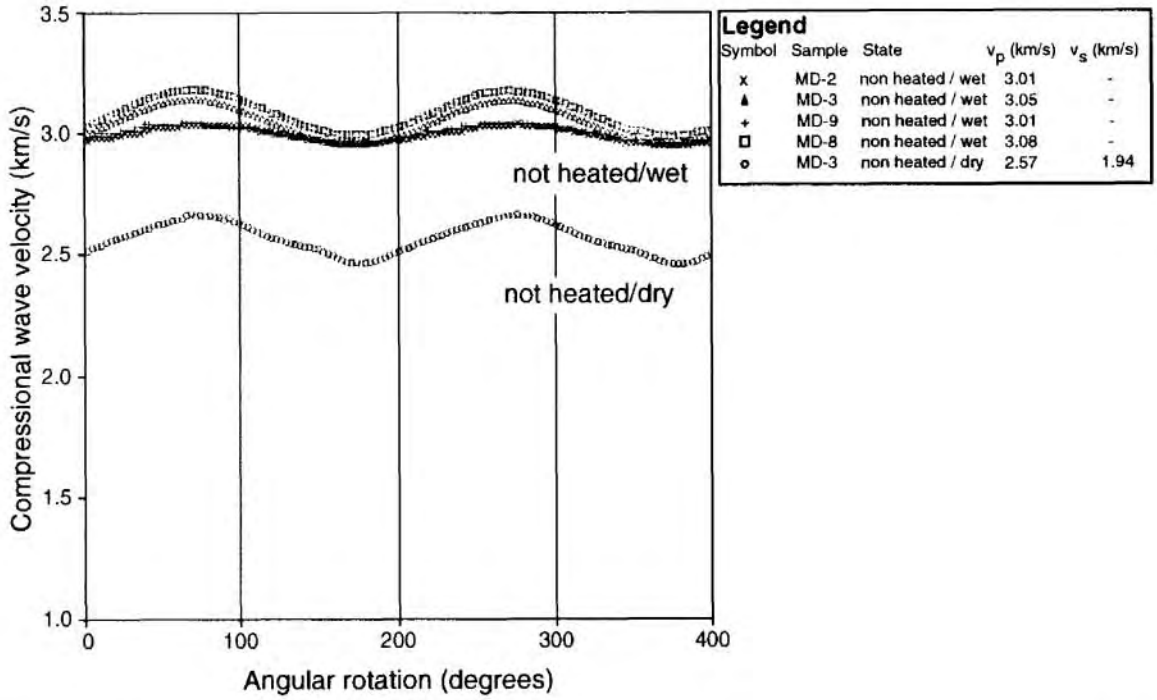


**Fig. 3a Ultrasonic compressional wave velocity of non-heated water-saturated ("wet") and non-heated "dry" Bentheim sandstone samples.**

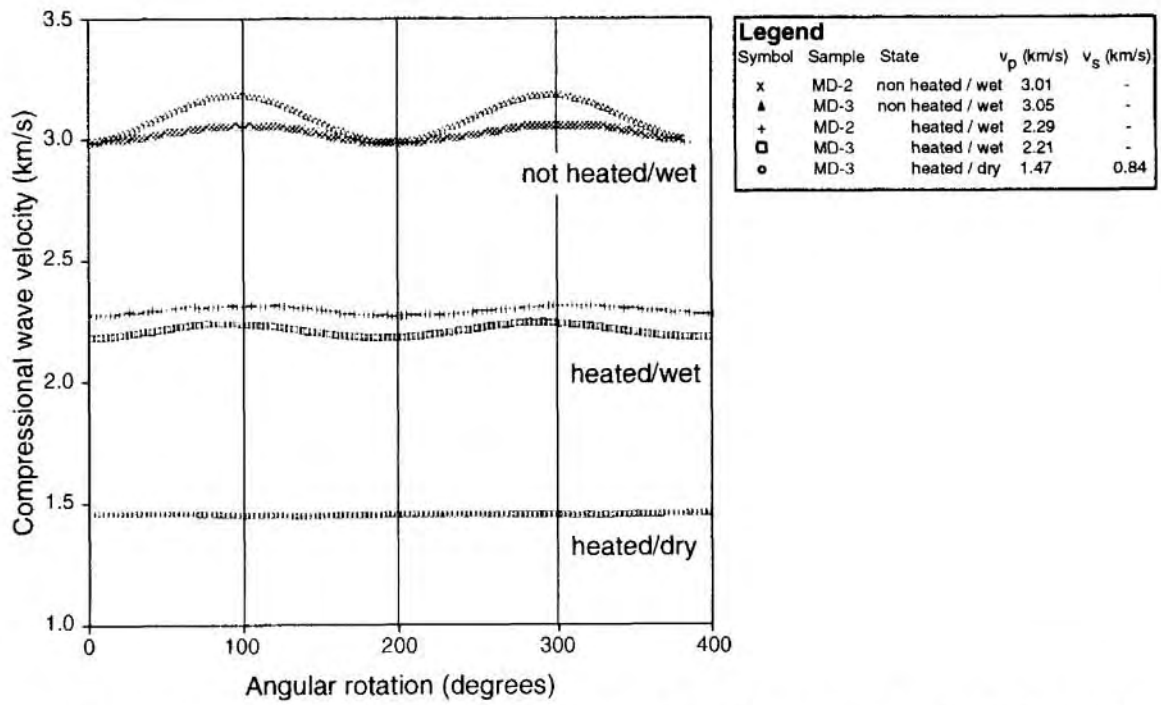


**Fig. 3b Ultrasonic compressional wave velocity of non-heated water-saturated ("wet"), heated "wet" and heated "dry" Bentheim sandstone samples.**

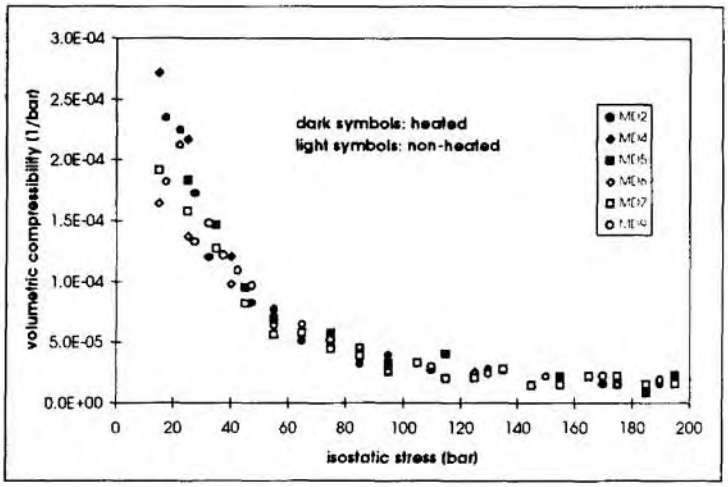


*Fig.4. Volumetric compressibility of non-heated and heated Bentheim sandstone as a function of isostatic stress up to 200 bar; from 200 up to 700 bar the data points for non-heated and heated samples overlap*

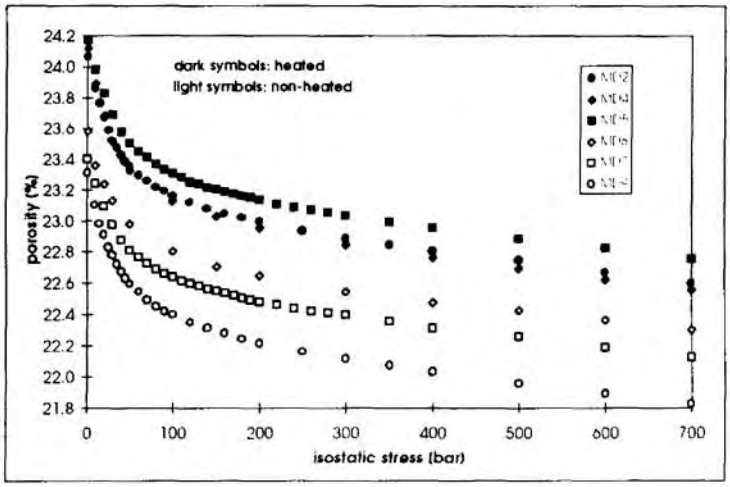


*Fig.5. Porosity of non-heated and heated Bentheim sandstone as a function of isostatic stress up to 700 bar*

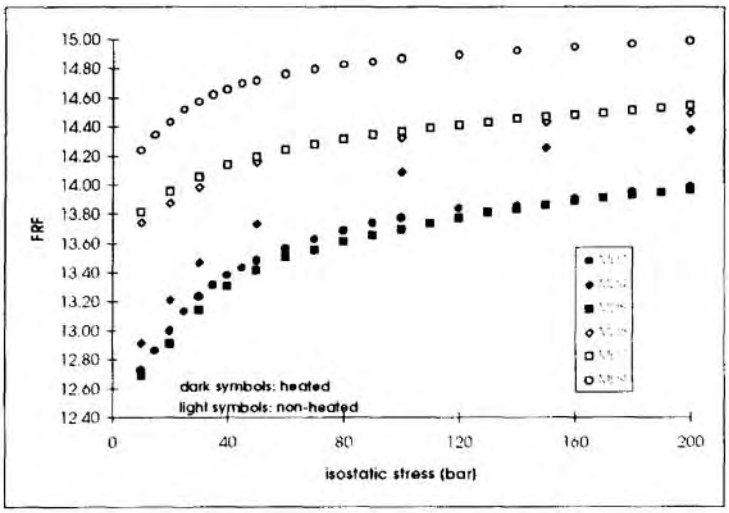


*Fig.6 Formation resistivity factor of heated and not heated Bentheim sandstone as a function of isostatic stress up to 200 bar; from 200 to 700 bar the data for heated and not heated samples show a similar trend*

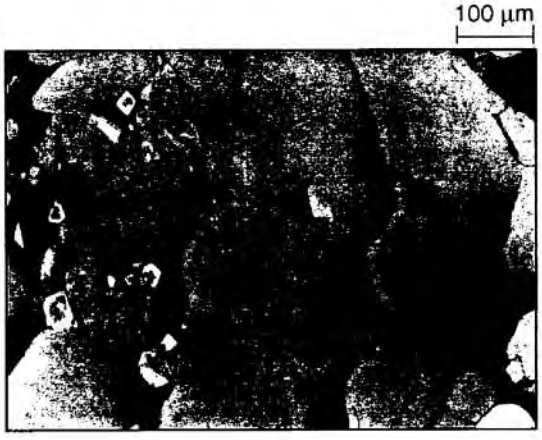


Fig. 7a Typical grain boundary morphology between quartz grains in the reservoir sandstone.

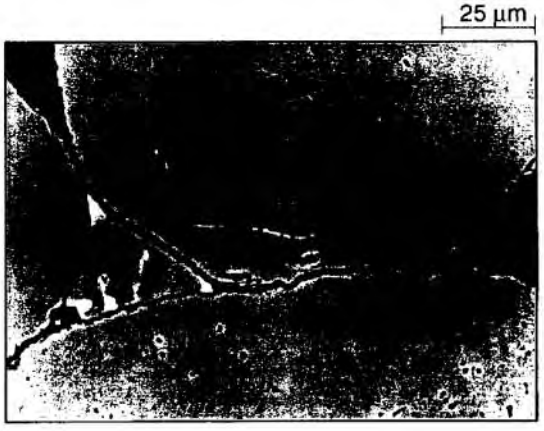


Fig. 7a Magnification of the central part of Fig. 7a.

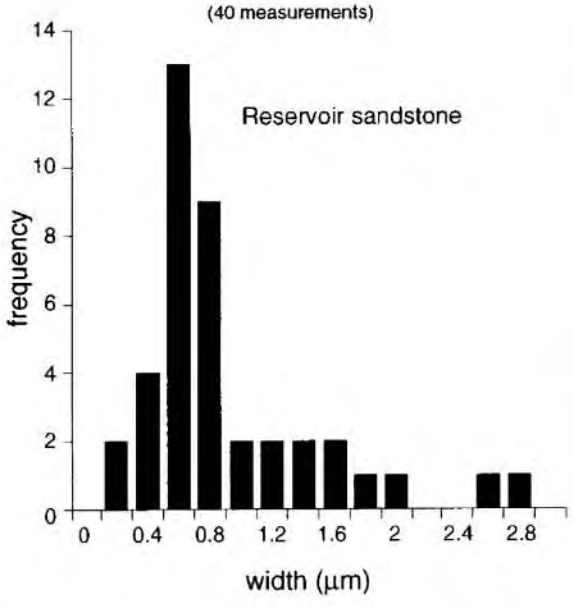


Fig. 8a Grain boundary width of the reservoir sandstone, measured from SEM photomicrographs; grain size 100 - 1000 µm.

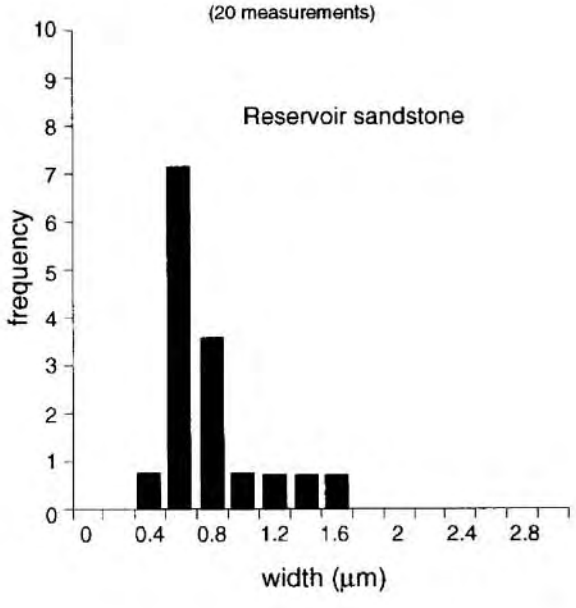


Fig. 8b Grain boundary width of the reservoir sandstone, measured from SEM photomicrographs; grain size 100 - 400 µm.